



Short communication

Intranasal immunization with recombinant Vaccinia virus encoding trimeric SARS-CoV-2 spike receptor-binding domain induces neutralizing antibody

Xiaoling Cao^{a,1}, Junjie Zai^{c,1}, Qingzhen Zhao^d, Lilan Xie^{a,b}, Yaoming Li^{a,b,*}

^a College of Life Science and Technology, Wuhan University of Bioengineering, Wuhan, China

^b Hubei Engineering Research Center of Viral Vector, Applied Biotechnology Research Center, Wuhan University of Bioengineering, Wuhan, China

^c Immunology Innovation Team, School of Medicine, Ningbo University, Ningbo, China

^d The Affiliated Hospital of Medical School, Ningbo University, Ningbo, China



ARTICLE INFO

Article history:

Received 15 March 2022

Received in revised form 1 August 2022

Accepted 23 August 2022

Available online 29 August 2022

Keywords:

Vaccinia virus

SARS-CoV-2

Trimeric RBD

Neutralization

ABSTRACT

Respiratory transmission of SARS-CoV-2 is considered to be the major dissemination route for COVID-19, therefore, mucosal immune responses have great importance in preventing SARS-CoV-2 from infection. In this study, we constructed a recombinant Vaccinia virus (VV) harboring trimeric receptor-binding domain (RBD) of SARS-CoV-2 spike protein (VV-_{trRBD}), and evaluated the immune responses towards RBD following intranasal immunization against mice and rabbits. In BALB/c mice, intranasal immunization with VV-_{trRBD} elicited robust humoral and cellular immune responses, with high-level of both neutralizing IgG and IgA in sera against SARS-CoV-2 pseudoviruses, and a number of RBD-specific IFN- γ -secreting lymphocytes. Sera from immunized rabbits also exhibited neutralization effects. Notably, RBD-specific secretory IgA (sIgA) in both nasal washes and bronchoalveolar lavage fluids (BALs) were detectable and showed substantial neutralization activities. Collectively, a recombinant VV expressing trimeric RBD confers robust systemic immune response and mucosal neutralizing antibodies, thus warranting further exploration as a mucosal vaccine.

© 2022 Elsevier Ltd. All rights reserved.

1. Introduction

The COVID-19 pandemic has made an unprecedented impact on human health and global economy. The causative agent SARS-CoV-2 belongs to *Coronavirus* family β , which also contains other two seriously infectious and highly deadly pathogens, SARS-CoV and MERS-CoV. Like other human coronaviruses, the full-length spike protein (S) of SARS-CoV-2 structurally consists of S1 and S2 subunits [1]. The S1 protein, specifically, the receptor-binding domain (RBD), mediates viral attachment to its receptor, human angiotensin-converting enzyme 2 (hACE2). The engagement of S1 protein-hACE2 in turn triggers the membrane fusion between virus and host cell, hence prompting the genetic RNA insertion into the host cell [2]. As antibody-mediated RBD-blocking may stymie the initial step of virus infection, RBD is considered to be a vulnerable

target and superior candidate immunogen. Indeed, a large panel of studies regarding RBD-based vaccines against SARS-CoV-2 have demonstrated RBD as an appealing vaccine candidate preventing animal from infection [3–7]. For instance, intramuscular immunization with various forms of RBD protein (e.g., monomer RBD, [3] Fc-fused or tandem-repeat dimer, [4,8,9] covalent trimer, [5] and nanoparticle-displayed multimer [6,7]) induced substantial protection upon various challenge models.

The attenuated Vaccinia virus tiantan strain (VV-_{TT}) as a vector has been widely used for novel vaccine development due to its outstanding safety and genetic stability [10–12]. More importantly, the large genome of VV is capable of accommodating several exogenous genes simultaneously, thus allowing new recombinant VV to be easily constructed. We demonstrated previously that monomeric SARS-CoV-2 RBD could be efficiently expressed when driven by the VV-specific promoter [13]. Here in the current study, we report construction and characterization of a recombinant VV stably expressing trimeric SARS-CoV-2 spike RBD. Afterwards, the humoral and cellular immune responses towards RBD were evaluated following intranasal administration in mice and rabbits.

* Corresponding author at: College of Life Science and Technology, Wuhan University of Bioengineering, Wuhan 430415, China.

E-mail addresses: zaijunjie@nbu.edu.cn (J. Zai), fyzhaoqingzhen@nbu.edu.cn (Q. Zhao), xielilan@webmail.hzau.edu.cn (L. Xie), limeming@webmail.hzau.edu.cn (Y. Li).

¹ These authors contributed equally to this work.

1.1. Characterization of recombinant Vaccinia virus expressing trimeric SARS-CoV-2 RBD

A 27-residue (GYIPEAPRDGQAYVRKDGWVLLSTFL) trimerization domain (glycosylphosphatidylinositol, GPI) derived from the C-terminal bacteriophage T4 fibrin [14] was fused with RBD (derived from SARS-CoV-2 WA1 strain) at C-terminus, ensuring the formation of trimeric RBD, namely tRBD. Specifically, the optimized DNA sequence (GGC UAC AUC CCU GAG GCU CCA CGC GAC GGA CAA GCC UAC GUC AGA AAG GAC GGA GAG UGG GUC UUA UUG UCU ACU UUC CUU) encoding GPI was synthesised *in vitro*, and seamlessly cloned to the 3'-terminal of RBD DNA sequence. To generate a recombinant VV expressing tRBD, the plasmid pLARA-tRBD carrying bidirectional expression cassettes of GFP and tRBD was constructed (Fig. 1A) and then transfected into the Vero-1008 cells that had already been infected with VV-TT. The fluorescent viral plaque was picked out and subject to a new round of infection and viral selection. After at least five rounds of purification, the resultant individual recombinant virus VV-tRBD was propagated and evaluated for its bio-features, including replication dynamic, genetic stability, and supportive capability for exogenous gene expression, with VV-CPV-VP2 [12] as an irrelative viral control. At 36 h post infection by VV-tRBD, Vero-1008 cells were subject to indirect fluorescent assay (IFA) and Western blot assay using RBD-specific nanobody H11-D4. [15] As shown in Fig. 1B, tRBD protein was visible in VV-tRBD-infected Vero-1008 cells, whereas VV-CPV-VP2-infected Vero-1008 displayed no red signal. As seen in Fig. 1C, no specific bands were detected for VV-CPV-VP2-infected Vero-1008 in denatured PAGE, whereas VV-tRBD-infected Vero-1008 yielded a specific band about 27 kD, a size consistent with predicted molecule weight of RBD. Interestingly, a much larger band (~45 kD) than expected, probably an as yet undefined modification of RBD like glycosylation, was also detected. After the Vero-1008 cells were infected by VV-tRBD or VV-TT for 36 h, the average diameters of VV-TT and VV-tRBD were also compared. As shown in Fig. 1D, the diameter of VV-tRBD plaque was not significantly shorter than that of VV-TT. ($p = 0.052$, student-*t* test) This experiment was individually performed five times. Lastly, the replication dynamics of Vero-1008 infected by either VV-TT or VV-tRBD were evaluated. As exhibited in Fig. 1E, both virus titers reached their peaks of the virus replication curve without apparent difference at 48 h post infection. Collectively, these data indicate a recombinant VV encoding trimeric RBD with comparable replication ratio to VV-TT was successfully developed.

Whether intranasal immunization of high-dose VV-tRBD has side effects on mice is another concern and should be addressed. To this end, five six-week female BALB/c mice were intranasally immunized with 1×10^7 plaque-forming unit (PFU) of VV-tRBD in 10 μ l (5 μ l per time, 15 min apart), followed by continuously monitoring body-weight for 14 days. As a control, five six-week female BALB/c mice were similarly treated with VV-TT. As shown in Fig. 1F, the body-weight of mice inoculated with 1×10^7 PFU of VV-tRBD dropped slightly at around day 4, and recovered promptly thereafter. In contrast, the bodyweight of VV-TT group mice decreased significantly at around day 6, although no mice died. To ascertain whether the slight decline of mice bodyweight was correlated to immunization regimen, nine 6-week BALB/c mice (three mice per group) were intranasally inoculated with 1×10^7 PFU of VV-tRBD, 1×10^7 PFU of VV-TT or PBS in 10 μ l (5 μ l per time, 15 min apart), respectively. Mouse lungs tissues were achieved at day 3 post immunization and analyzed for possible histology damage due to the intranasal administration by HE staining. As shown in Fig. 1G, no obvious lung tissue injury can be found in either VV-tRBD or VV-TT mice group. Therefore, the current dose of VV-tRBD ought to be highly safe for mice via intranasal immunization.

1.2. Systemic and mucosal binding antibody for RBD

In order to evaluate the immunogenicity of VV-tRBD, systemic and mucosal antibodies toward RBD were determined following intranasal immunization. The animal immunization was scheduled as indicated in diagram. (Fig. 2A) Specifically, after complete anaesthesia with pentobarbital sodium, three groups of six-week female BALB/c mice (five mice per group) were intranasally vaccinated with 2×10^6 PFU (low-dose) or 1×10^7 PFU (high-dose) of VV-tRBD in 10 μ l (5 μ l per time, 15 min apart), or 1×10^7 PFU of VV-CPV-VP2 in 10 μ l (5 μ l per time, 15 min apart), respectively, with VV-CPV-VP2 group as control. The fourth mice group (five six-week female BALB/c mice) was intracutaneously immunized with 1×10^7 PFU of VV-tRBD in 10 μ l. All the mice were immunized twice, 30 days apart. The blood samples were collected from the retro-orbital plexus at day10 post booster immunization, meanwhile the mucosal samples were also obtained. Then the RBD-specific antibody titers were assessed by ELISA. As shown in Fig. 2B, end-point titer (EPT) of sera from mice receiving high-dose VV-tRBD reached 12,400 (IgG titer) [95 % CI, 11,200 to 13,600], while low-dose group gained sera EPT of 9,600 [95 % CI, 8,750 to 12,300]; The IgA titers in sera reached 713 [95 % CI, 854 to 555] and 164 [95 % CI, 65 to 256] in high- and low-dose group, respectively. (Fig. 2C) Meanwhile, intracutaneous immunization induced high level of humoral immune response, with RBD-specific sera IgG and IgA titers reaching 21,500 [95 % CI, 19,760 to 22,320] and 679 [95 % CI, 265 to 985], respectively. The EPTs of sera IgG and IgA were significantly different between the high- and low-dose VV-tRBD groups. ($p < 0.05$) (Fig. 2B and 2C) In contrast, neither RBD-specific IgG nor IgA were detectable in sera from VV-CPV-VP2 control group mice.

Since intranasal immunization is thought to develop mucosal-skewed immune response, antibody titers of mucosal secreted IgA (sIgA) against RBD were examined in mice. Briefly, saliva was collected following carbachol treatment at day 10 post booster immunization. After sacrifice, mouse nasal washes and vaginal lavage fluids were obtained by rinsing the nasal cavity and vaginal tract respectively with 40 μ l of sterile PBS; mouse bronchoalveolar lavage fluids (BALs) were acquired by washing the entire pulmonary lumen with 100 μ l of PBS. Totally-three times were performed for all these washings. Then, 100 μ l of mucosal samples were serially diluted 4-fold for ELISA. As seen in Fig. 2D, the high- and low-dose group had a RBD-specific EPT IgA titers from saliva of 35 [95 % CI, 26 to 56] and 13 [95 % CI, 9 to 15]. In addition, RBD-specific mucosal sIgA titers from high-dose group in vaginal lavage fluids, nasal washes; and BALs in high-dose group reached 142 [95 % CI, 126 to 158], 67 [95 % CI, 57 to 84] and 29 [95 % CI, 23 to 32], respectively. The endpoint sIgA titers were significantly different between the high- and low-dose VV-tRBD groups. ($p < 0.05$) (Fig. 2E to 2G) However, the RBD-specific mucosal sIgA titers were extremely low in mucosal samples from the intracutaneously immunized mice. In contrast, RBD-specific sIgA was undetectable in all the mucosal samples, such as saliva, vaginal lavage fluids, nasal washes, and BALs, from mice in VV-CPV-VP2 control group.

Following the same immunization regimen for mice mentioned above, three groups of rabbits were vaccinated (five female rabbits per group), then bled from auricular vein at day 10 post booster immunization for evaluation of RBD-specific sera IgG and IgA titers. As shown in Fig. 2H, rabbits receiving high-dose VV-tRBD gained sera EPT of 8,450 [95 % CI, 6,870 to 9,760] (IgG titer), meanwhile, the low-dose group EPT reached 3,120 [95 % CI, 2,643 to 3,670]. In contrast, the sIgA titer in sera was quantified to be 274 [95 % CI, 245 to 297] and 81 [95 % CI, 56 to 112] in high- and low-dose groups, respectively. (Fig. 2I) Collectively, these results support that intranasal immunization VV-tRBD can elicit marked RBD-binding antibody in sera from both mice and rabbits in a

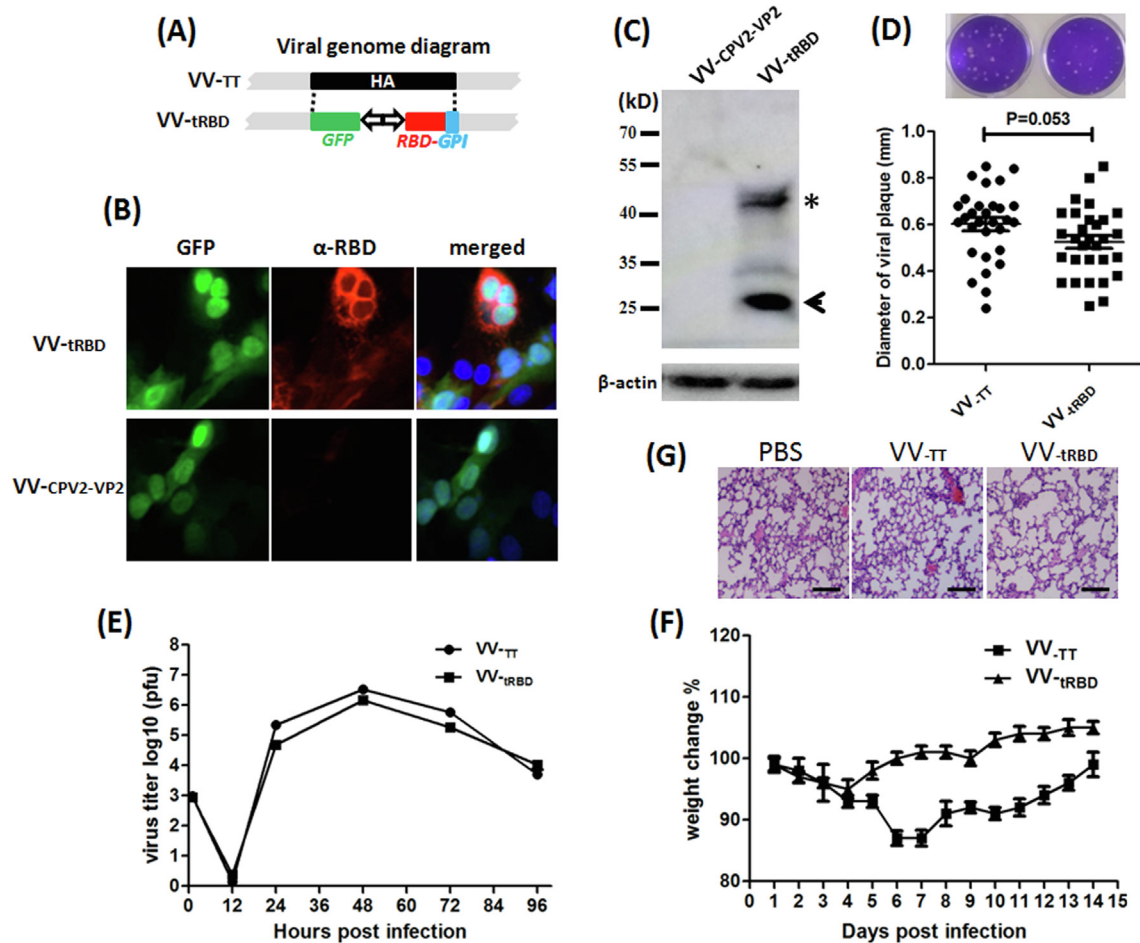


Fig. 1. Characterization of VV-IRBD. (A) Diagram of developing VV-IRBD. VV-TT HA gene was replaced by two open reading frames (ORFs) *gfp* and SARS-CoV-2 *tRBD* in opposite direction that were driven by two promoters, forming a new recombinant Vaccinia virus (VV-IRBD). (GPI, glycosylphosphatidylinositol) The *gfp* serves as a fluorescent selection marker for recombinant VV. (B–C) The RBD expression analysis. Vero-1008 cells were infected with VV-IRBD or VV-CPV2-VP2, respectively. At 36 h post infection, Vero-1008 cells were subject to indirect fluorescent assay (IFA) (B) and Western blotting (C) using RBD-specific nanobody H11-D4. The arrow head indicates RBD band. The asterisk indicates a possibly modified RBD. VV-CPV2-VP2 serves as an irrelative recombinant virus control. (D) Comparison of viral plaques diameters. Vero-1008 cells were infected with VV-IRBD or VV-TT, respectively. At 36 h post infection, Vero-1008 cells were subject to fixation by 4 % paraformaldehyde and crystal violet cell staining *in situ*. Following complete washing with water, diameters of thirty viral plaques were recorded and the mean values of diameter of VV-TT and VV-IRBD were calculated and compared. This experiment was individually performed five times. (E) The kinetics of VV-IRBD replication. Vero-1008 cells were infected with VV-IRBD or VV-TT at an MOI of 0.01, respectively. At 0, 12, 24, 48, 72 and 96 h post infection, Vero-1008 was collected and subject to virus plaque assay to quantify the virus plaque numbers. (F) Five 6-week-old BALB/c mice were intranasally inoculated with 1×10^7 PFU of VV-IRBD, and the bodyweight were monitored daily for 14 days post infection. Another five mice was treated with same amount of VV-TT as a control group. (G) Nine 6-week BALB/c mice (three mice per group) were respectively intranasally inoculated with 1×10^7 PFU of VV-IRBD, VV-TT or PBS in 10 μ l (5 μ l per time, 15 min apart). The lung tissues from intranasally administrated mice at day 3 post inoculation were analyzed for possible histology damage due to the intranasal administration by HE staining. Bar: 50 μ m. (For interpretation of the references to colour in this figure legend, the reader is referred to the web version of this article.)

dose-dependent manner. Notably, RBD-specific binding mucosal sIgAs were detectable in VV-IRBD-vaccinated mice intranasally instead of intracutaneously.

1.3. Neutralizing antibody towards SARS-CoV-2 pseudoviruses

In order to assess the neutralization capacity, sera and mucosal samples were obtained from immunized mice and evaluated using pseudovirus neutralization assay. The sera were obtained and subject to 25-fold serial dilution and evaluated for the neutralization effects against SARS-CoV-2 pseudoviruses at day 10 post booster immunization. Two SARS-CoV-2 pseudoviruses (HIV-1 backbone), which were packaged with spike protein from SARS-CoV-2 strain WA1 and the current Omicron (B.1.1.529) variant of concern (VOC), respectively, were used to assess the cross-neutralizing potency of sera or mucosal samples. As shown in Fig. 3A, sera from high- and low-dose VV-IRBD-immunized mice group effectively neutralized the WA1 pseudovirus, with a 50 % neutralization titer (NT₅₀) of 356 [95 % CI, 245 to 478] and 176 [95 % CI, 145 to 213],

whereas the neutralization effects of mice sera towards Omicron pseudovirus (B.1.1.529) decreased sharply, with a NT₅₀ of 112 [95 % CI, 57 to 136] and 43 [95 % CI, 27 to 76], respectively, which was consistent with recent reports by other groups. [16,17] In contrast, the control sera did not show any neutralization effect even at the minimum dilution tested (1:25). Intriguingly, intracutaneous immunization with VV-IRBD induced substantial sera neutralizing antibody as well, with a NT₅₀ of 487 [95 % CI, 342 to 523] and 95 [95 % CI, 76 to 112] to WA1 and Omicron, respectively.

With the same method mentioned above, sera from immunized rabbits were also evaluated for the neutralization effect against the two pseudoviruses. As observed in Fig. 3B, VV-IRBD-immunized rabbits effectively neutralized WA1 pseudoviruses, with a NT₅₀ of 190 and 96, respectively. Unfortunately, all the sera from rabbits did not show any neutralization effect against Omicron pseudovirus (B.1.1.529).

Furthermore, we investigated whether mucosal samples from mice could neutralize SARS-CoV-2 pseudoviruses. As seen in Fig. 3C to 3F, saliva, vaginal lavage fluids, nasal washes, and BALs

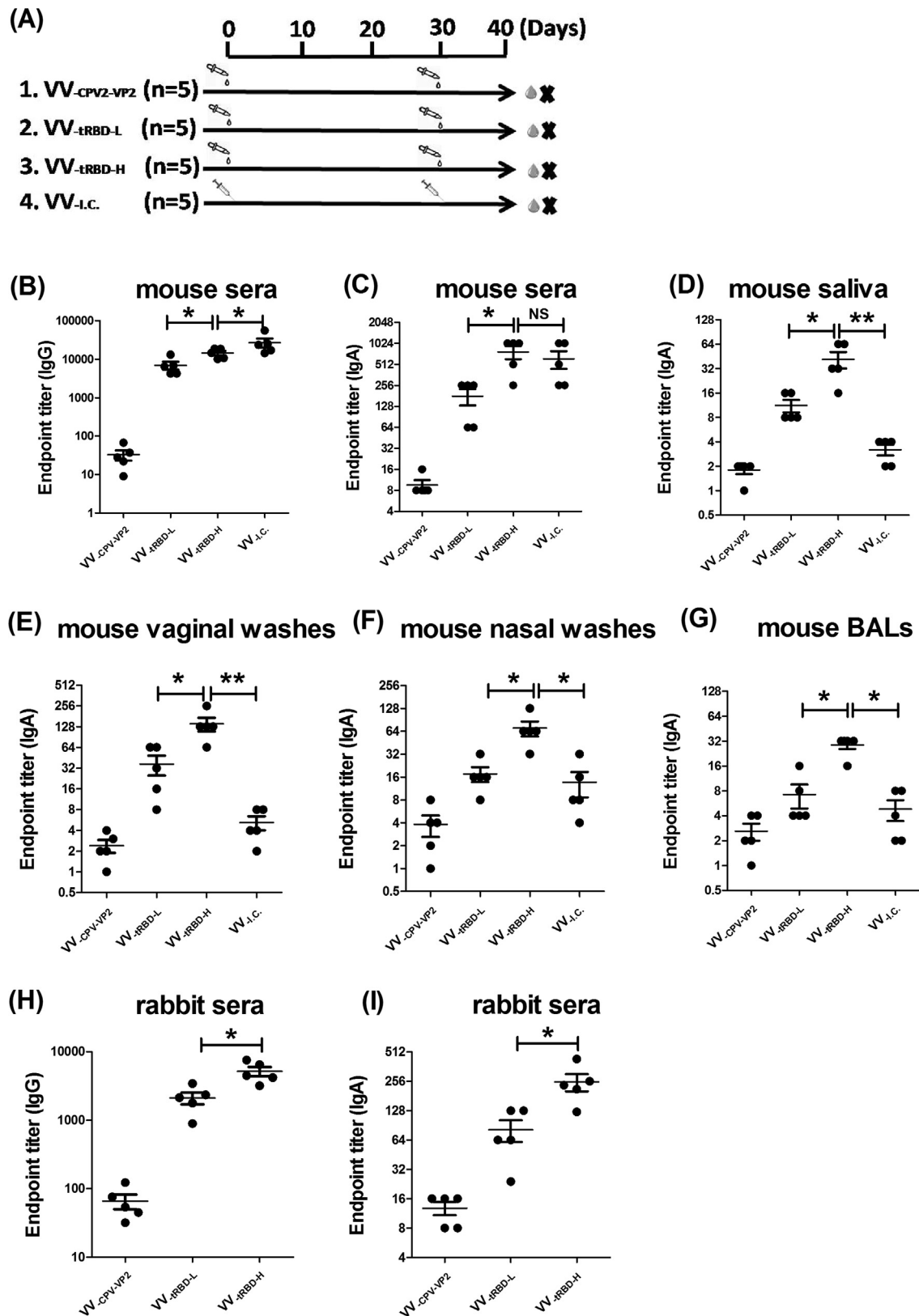


Fig. 2. RBD-specific binding antibody. Four groups (5 mice per group) of mice were intranasally immunized with 2×10^6 PFU (low-dose VV-_{IRBD}, VV-_{IRBD-L}) in 10 μ l (5 μ l per time, 15 min apart), 1×10^7 PFU (high-dose VV-_{IRBD}, VV-_{IRBD-H}) of VV-_{IRBD} in 10 μ l (5 μ l per time, 15 min apart), 1×10^7 PFU of VV-CPV2-VP2 in 10 μ l (5 μ l per time, 15 min apart), or intracutaneously immunized with 1×10^7 PFU of VV-_{IRBD} in 10 μ l, respectively. All the mice were immunized twice with an interval of 30 days. **(A)** Immunization groups and regimens. The blood samples were collected from the *retro*-orbital plexus at day 10 post booster immunization, and then the RBD-specific sera IgG **(B)** and IgA **(C)** were assessed by ELISA. Saliva was collected after carbachol treatment. Mouse nasal washes and vaginal lavage fluids were obtained by rinsing the nasal cavity and vaginal tract respectively with 40 μ l of sterile PBS; Bronchoalveolar lavage fluids (BALs) were acquired by washing the entire pulmonary lumen with 100 μ l of PBS. Totally-three times were performed for all these washings. Then, 100 μ l of mucosal samples were serially diluted 4-fold for ELISA to determine the sIgA titers in saliva **(D)**, vaginal washes **(E)**, nasal washes **(F)**, and BALs **(G)**, respectively. With the same immunization schedule mentioned above for mice, three groups of rabbits were vaccinated and bled from auricular vein. The RBD-specific sera IgG **(H)** and IgA **(I)** titers were determined using ELISA. (*, $p < 0.05$; **, $p < 0.01$; Oneway ANOVA).

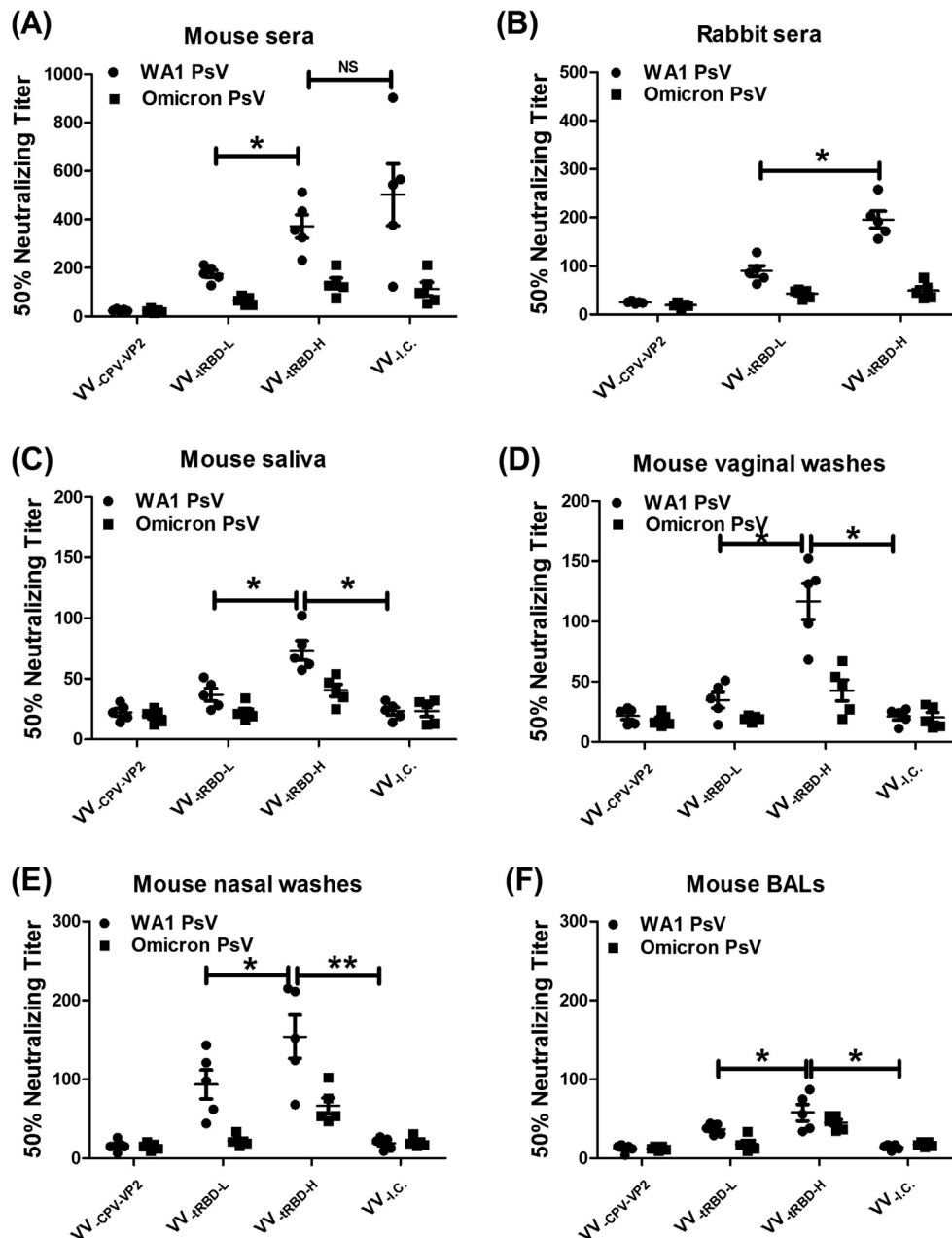


Fig. 3. Neutralization effects of sera and mucosal samples. Neutralizing antibodies in sera and mucosal samples from mice intranasally immunized with VV-CPV-VP2, VV-IRBD-L, VV-IRBD-H, or mice intracutaneously immunized with VV-I.C. were assessed by pseudovirus neutralization assay. VV-CPV-VP2, low-dose VV-IRBD (2×10^6 PFU); VV-IRBD-H, high-dose VV-IRBD (1×10^7 PFU); VV-CPV-VP2, (1×10^7 PFU); and VV-I.C., intracutaneous VV-IRBD (1×10^7 PFU). Sera from mice (A) or rabbits (B) were immunized with indicated recombinant virus assessed by two SARS-CoV-2 pseudoviruses (WA1 and Omicron (B.1.1.529) PsV). With the same method, the neutralization effects of mucosal samples, including saliva (C), vaginal lavage fluid (D), nasal washes (E), and BALs (F) from mice immunized with indicated recombinant virus were also evaluated using two SARS-CoV-2 pseudoviruses (WA1 and Omicron (B.1.1.529) PsV). (*, $p < 0.05$; **, $p < 0.01$; Oneway ANOVA).

from only high-dose VV-IRBD-immunized mice showed limited neutralization effect to WA1 instead of Omicron (B.1.1.529) pseudovirus, with a NT₅₀ of 64 [95 % CI, 57 to 86], 106 [95 % CI, 77 to 124], 146 [95 % CI, 121 to 154] and 58 [95 % CI, 43 to 74], respectively. In contrast, the saliva, vaginal lavage fluids, and BALs from control group mice did not show any neutralization effect to either pseudovirus even at the minimum dilution tested (1:25). Despite intracutaneous administration of VV-IRBD induced comparable level of sera IgG to that by intranasal inoculation ($p > 0.05$), RBD-specific mucosal sIgA could not be detected following intracutaneous administration. Overall, high-dose VV-IRBD elicited high-level of neutralizing antibodies (IgG and IgA) in sera, and limited but effec-

tive sIgA in mucosa, against SARS-CoV-2 pseudoviruses following intranasal instead of intracutaneous administration.

1.4. Cellular immune responses

Given the critical roles of cytokines secreted by activated immunocytes in defining the subsequent immune response, [18] we assessed SARS-CoV-2 RBD-specific Th1-, Th2-, or Th17-like cellular immune responses by measuring the production of Th1-associated (IFN- γ), Th2-associated (IL-4), or Th17-associated (IL17a) cytokines. Splenocytes collected from immunized mice at day 10 post booster immunization were stimulated with pur-

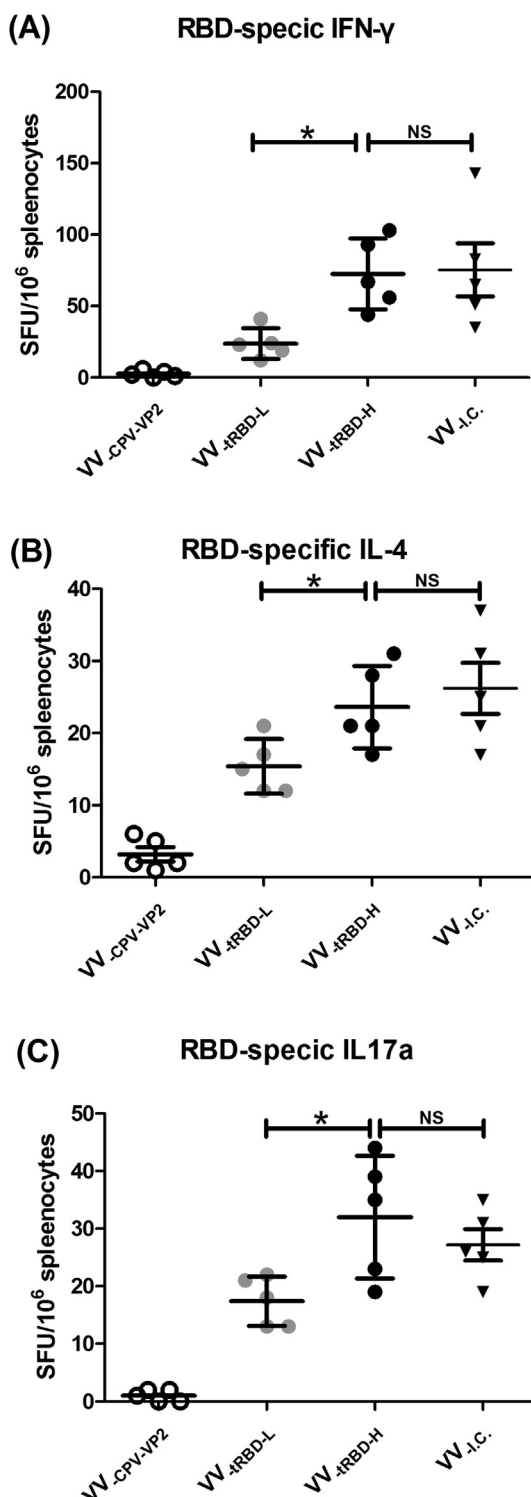


Fig. 4. Cellular immune responses. At 10 days post final immunization, splenocytes from mice immunized with indicated recombinant VVs were isolated with Ficoll-Paque, followed by stimulation with whole RBD protein in 96-well plate. RBD-specific IFN- γ (A), IL-4 (B) or IL17-secreting T cells (C) were analyzed by ELISPOT. VV-IRBD-L, low-dose VV-IRBD (2×10^6 PFU); VV-IRBD-H, high-dose VV-IRBD (1×10^7 PFU); VV-CPV-VP2, 1×10^7 PFU; and VV-ILC, intracutaneous VV-IRBD (1×10^7 PFU). Cytokine-secreting cells forming or accounting were performed according to the manufacturers' instructions. (*, $p < 0.05$; One way ANOVA).

chased RBD protein (SinoBiological, CN) and analyzed using ELISPOT (enzyme linked immunospot assay). As shown in Fig. 4A, splenocytes from mice in VV-CPV-VP2 group did not produce any

detectable immunocytes secreting IFN- γ , IL-4, and IL17a, whereas the amount of SARS-CoV-2 RBD-specific IFN- γ -secreting T cells reached an average of 26 [95 % CI, 17 to 36], 75 [95 % CI, 59 to 92], and 78 [95 % CI, 65 to 89] spot-forming cells (SFC) per million splenocytes from mice intranasally immunized with low-, high-dose VV-IRBD and mice intracutaneously immunized with 1×10^7 PFU of VV-IRBD, respectively. In contrast, the amount of RBD-specific IL4- or IL17a-secreting T cells from mice vaccinated by high-dose VV-IRBD was only about 24 [95 % CI, 14 to 35] and 32 [95 % CI, 23 to 46], respectively, indicating that the amounts of RBD-specific IL4- or IL17a-secreting T cells are significantly different between the high- and low-dose VV-IRBD groups. ($p < 0.05$, One-way ANOVA) While intracutaneous administration of VV-IRBD induced comparable amount of RBD-specific IL4- or IL17a-secreting T cells with intranasal inoculation. (Fig. 4B and 4C) ($p > 0.05$) Therefore, both intranasal and intracutaneous immunization with VV-IRBD seemed to induce a Th1-dominant cellular response, with much more immunocytes secreting IFN- γ than the other two immunocytes secreting IL-4 and IL17a.

Compared to conventional SARS-CoV-2 vaccines, the candidate vaccine studied here showed marked benefits. Firstly, individual SARS-CoV-2 RBD exhibits low immunogenicity due to its relatively low molecule weight (~ 27 kD), while polymerization of RBD, such as dimerization, trimerization, or poly-displayed on nanoparticle, can significantly promote the immunogenicity [3–5,9]. In the current study, we used GPI to trimerize RBD, thus to mimic the native structure and enhance its immunogenicity. Secondly, muscular immunization of a protein-based vaccine, generally, tends to induce systemic immune responses, whereas mucosal immunization can stimulate both mucosal and systemic immune responses. For SARS-CoV-2, respiratory tract is thought to be the major route for virus transmission between human to human [19]. Our data showed that mucosal immune response can be elicited, which therefore raised feasibility for first defense against SARS-CoV-2 infection. And thirdly, VV-based recombinant virus can efficiently induce high-level of cellular immunity that is also considered important for intracellular virus clearance [20]. Altogether, recombinant VV expressing SARS-CoV-2 RBD in trimer form provides a promising vaccine candidate preventing SARS-CoV-2 from infection via mucosal immunization.

Data availability

Data will be made available on request.

Declaration of Competing Interest

The authors declare that they have no known competing financial interests or personal relationships that could have appeared to influence the work reported in this paper.

Acknowledgements

This work was supported by grants from National Natural Science Foundation of China (No. 31972692), Hubei Provincial Natural Science Foundation of China (No. 2020CFB520), Natural Science Foundation of Ningbo (No. 202003N4010), Natural Science Foundation of Zhejiang (No. LGF21C010001).

References

- [1] Yan R, Zhang Y, Li Y, Xia L, Guo Y, Zhou Q. Structural basis for the recognition of SARS-CoV-2 by full-length human ACE2. *Science* 2020;367(6485):1444–8.
- [2] Shang J, Wan Y, Luo C, Ye G, Geng Q, Auerbach A, et al. Cell entry mechanisms of SARS-CoV-2. *Proc Natl Acad Sci U S A* 2020;117(21):11727–34.

- [3] Yang J, Wang W, Chen Z, Lu S, Yang F, Bi Z, et al. A vaccine targeting the RBD of the S protein of SARS-CoV-2 induces protective immunity. *Nature* 2020;586(7830):572–7.
- [4] Liu Z, Xu W, Xia S, Gu C, Wang X, Wang Q, et al. RBD-Fc-based COVID-19 vaccine candidate induces highly potent SARS-CoV-2 neutralizing antibody response. *Signal Transduct Target Ther* 2020;5(1).
- [5] Routhu NK, Cheedarla N, Bollimpelli VS, Gangadhara S, Edara VV, Lai L, et al. SARS-CoV-2 RBD trimer protein adjuvanted with Alum-3M-052 protects from SARS-CoV-2 infection and immune pathology in the lung. *Nat Commun* 2021;12(1).
- [6] Tan TK, Rijal P, Rahikainen R, Keeble AH, Schimanski L, Hussain S, et al. A COVID-19 vaccine candidate using SpyCatcher multimerization of the SARS-CoV-2 spike protein receptor-binding domain induces potent neutralising antibody responses. *Nat Commun* 2021;12(1).
- [7] Cohen AA, Gnanaprasam PNP, Lee YE, Hoffman PR, Ou S, Kakutani LM, et al. Mosaic nanoparticles elicit cross-reactive immune responses to zoonotic coronaviruses in mice. *Science* 2021;371(6530):735–41.
- [8] Liu Z, Chan J-W, Zhou J, Wang M, Wang Q, Zhang G, et al. A pan-sarbecovirus vaccine induces highly potent and durable neutralizing antibody responses in non-human primates against SARS-CoV-2 Omicron variant. *Cell Res* 2022;32(5):495–7.
- [9] Xu K, An Y, Li Q, Huang W, Han Y, Zheng T, et al. Recombinant chimpanzee adenovirus AdC7 expressing dimeric tandem-repeat spike protein RBD protects mice against COVID-19. *Emerg Microbes Infect* 2021;10(1):1574–88.
- [10] Zhang Z, Dong L, Zhao C, Zheng P, Zhang X, Xu J. Vaccinia virus-based vector against infectious diseases and tumors. *Hum Vaccin Immunother* 2021;17(6):1578–85.
- [11] Xie L, Zai J, Yi K, Li Y. Intranasal immunization with recombinant Vaccinia virus Tiantan harboring Zaire Ebola virus gp elicited systemic and mucosal neutralizing antibody in mice. *Vaccine* 2019;37(25):3335–42.
- [12] Zhao W, Wang X, Li Y, Li Y. Administration with Vaccinia Virus Encoding Canine Parvovirus 2 vp2 Elicits Systemic Immune Responses in Mice and Dogs. *Viral Immunol* 2020;33(6):434–43.
- [13] Xie L, Yi K, Li Y. SARS-CoV2 RBD gene transcription cannot be driven by CMV promoter. *Virology* 2021;558:22–7.
- [14] Tao Y, Strelkov SV, Mesyanzhinov VV, Rossmann MG. Structure of bacteriophage T4 fibrin: a segmented coiled coil and the role of the C-terminal domain. *Structure* 1997;5(6):789–98.
- [15] Huo J, Le Bas A, Ruza RR, Duyvesteyn HME, Mikolajek H, Malinauskas T, et al. Neutralizing nanobodies bind SARS-CoV-2 spike RBD and block interaction with ACE2. *Nat Struct Mol Biol* 2020;27(9):846–54.
- [16] Cameroni E, Bowen JE, Rosen LE, Saliba C, Zepeda SK, Culap K, et al. Broadly neutralizing antibodies overcome SARS-CoV-2 Omicron antigenic shift. *Nature* 2022;602(7898):664–70.
- [17] Fang FF, Shi PY. Omicron: a drug developer's perspective. *Emerg Microbes Infect* 2022;11(1):208–11.
- [18] Yan Y, Hu K, Deng Xu, Guan X, Luo S, Tong L, et al. Immunization with HSV-2 gB-CCL19 Fusion Constructs Protects Mice against Lethal Vaginal Challenge. *J Immunol* 2015;195(1):329–38.
- [19] Focosi D, Maggi F, Casadevall A. Mucosal Vaccines, Sterilizing Immunity, and the Future of SARS-CoV-2 Virulence. *Viruses* 2022;14(2):187.
- [20] Moss P. The T cell immune response against SARS-CoV-2. *Nat Immunol* 2022;23(2):186–93.